RESEARCH ARTICLE

Synergistic Effects of PectaSol-C Modified Citrus Pectin an Inhibitor of Galectin-3 and Paclitaxel on Apoptosis of Human SKOV-3 Ovarian Cancer Cells

Ghamartaj Hossein[1]*, Maryam Keshavarz[1], Samira Ahmadi[1], Nima Naderi[2]

Abstract

Galectin-3 (Gal-3) is a carbohydrate-binding protein which is thought to be involved in cancer progression but its contribution to epithelial ovarian cancer (EOC) remains unclear. The present study sought to determine the role of Gal-3 in chemoresistance of the human SKOV-3 ovarian cancer cell line to paclitaxel (PTX) using recombinant human Gal-3 (rhGal-3) and PectaSol-C modified citrus pectin (Pect-MCP) as a specific Gal-3 competitive inhibitor. Our results showed 41% increased cell proliferation, 36% decreased caspase-3 activity and 33.6% increased substrate-dependent adhesion in the presence of rhGal-3 compared to the control case ($p<0.001$). Treatment of cells with a non-effective dose of PTX (100nM) and 0.1% Pect-MCP in combination revealed synergistic cytotoxic effects with 75% reduced cell viability and subsequent 3.9-fold increase in caspase-3 activity. Moreover, there was 39% decrease in substrate-dependent adhesion compared to control ($p<0.001$). These results suggest that inhibition of Gal-3 could be a useful therapeutic tool for combination therapy of ovarian cancer.

Keywords: Combination therapy - ovarian cancer - galectin-3 - modified citrus pectin - paclitaxel - apoptosis

Asian Pac J Cancer Prev, **14 (12)**, 7561-7568

Introduction

Epithelial ovarian cancer (EOC) remains one of the most common death in gynecological malignancy (Jemal et al., 2006). Paclitaxel (PTX), a potent drug of natural origin isolated from the bark of the Pacific yew, Taxus brevifolia (Wani et al., 1971), is currently used in the treatment of ovarian, lung, and breast cancer. Initial studies on the mechanism of action of taxol have demonstrated that this drug alters microtubule (MT) assembly, by inhibiting MT depolymerization and changing MT dynamics. These effects result in the disruption of the normal reorganization of the MT network required for mitosis and cell proliferation (Ahn et al., 2004). Although EOC are highly responsive to initial taxan-carboplatin-based combination chemotherapy, successful management of advanced or recurrent gynecological malignancies is often difficult because of both intrinsic and acquired resistance of cancer cells to cytotoxic drugs (Bae et al., 2009; Banerjee and Gore, 2009; Chumworathayi, 2013), thus, investigations for increased sensitivity to chemotherapy are needed for EOC patient.

Galectin-3 (Gal-3) is a 31KD carbohydrate-binding protein involved in growth, adhesion, migration, invasion and apoptosis of cancerous cells (Inohara et al., 1998; O'Driscoll et al., 2002; Nangia-Makker et al., 2007). Carbohydrate recognition domain (CRD) of Gal-3 is connected to a long proline- and glycine-rich NH2-terminal domain. This characteristic is unique among galectins and may be responsible for the interest in Gal-3 as a target molecule (Elola et al., 2007).The anti-apoptotic function of Gal-3 has been well demonstrated in variety of human cancers, such as breast, bladder and prostate (Choi et al., 2004; Oka et al., 2005; Wang et al., 2010). It has been demonstrated that Gal-3 knockout in PC3 prostate cancer cells could sensitize cells to chemotherapeutic drugs (Wang et al., 2010). Another reports showed that inhibition of Gal-3 could lead to increased cytotoxic effect of PTX in human colon cancer (Glinsky et al., 2009). In liver cancer Gal-3 inhibition induced apoptotic mitochondrial pathway and sensitize cells to chemotherapeutic drugs (Wongkham et al., 2009). Previous studies explained that Gal-3 effect on responsiveness of cancerous cells to antineoplastic drugs could be mediated by overcoming anoikis pathway (Kim et al., 1999; Zhao et al., 2010).

PectaSol-C modified citrus pectin (Pect-MCP) is a PH-/temperature-modified form of citrus pectin (CP). It is a highly complex branched polysaccharide rich in galactoside residues (Yan and Katz, 2010). CP is water insoluble and is unable to interact with Gal-3, but MCP is water soluble and acts as a ligand for Gal-3, competing with its association to natural ligands (Platt and Raz, 1992; Inohara and Raz, 1994; Pienta et al., 1995) It was reported that Pect-MCP could induce apoptosis and sensitize

*[1]Department of Animal Physiology, Developmental Biology Laboratory, School of Biology, University College of Science, University of Tehran, [2]Neuroscience Research Center, Shahid Beheshti University of Medical Sciences, Tehran, Iran *For correspondence: ghossein@khayam.ut.ac.ir*

prostate cancer cells to chemotherapeutic drugs (Wang et al., 2010; Tehranian et al., 2012).

There are controversial reports regarding Gal-3 expression and its role in EOC. One study reported down-regulation of Gal-3 expression in EOC compared to normal ovary (van den Brûle et al., 1994). However, other studies showed significant high levels of Gal-3 in the sera of ovarian cancer patients (Iurisci et al., 2000) and in EOC specimens compared to normal ovarian tissues (Kim et al., 2011). SKOV-3 cells are PTX resistant and transfection of these cells with Gal-3 siRNA led to enhanced cytotoxic effect of PTX on these cells (Kim et al., 2011). This study for the first time sought to determine the effect of recombinant human Gal-3 and Pect-MCP on proliferation, apoptosis, adhesion and chemoresistance of human ovarian cancer cell line SKOV-3.

Materials and Methods

Cell line and reagents

Human ovarian cancer SKOV-3 cells were a kind gift from Dr. A.H. Zarnani (Avicenna research center, Tehran, Iran). Cells were grown in Roswell Park Memorial Institute (RPMI)-1640 medium supplemented with 10% fetal bovine serum (FBS) and Penicillin/streptomycin antibiotics obtained from Life Technologies GmbH (Darmstadt, Germany) at 37°C in 5%CO_2 atmosphere under 90-95% humidity. 3-(4,5 dimethylthiazol-2yl)2,5diphenyltetrazolium bromide (MTT) and propodium iodide were obtained from Sigma-Aldrich (SaintLouis,USA), Ribonuclease A (iNtRON Biotechnology, Seoul, Korea), Paclitaxel was obtained from Stragen (Switzerland), Caspase-3 coloremetric assay kit was purchased from GenScript (NJ, USA) and RT-PCR reagents were provided by iNtRON Biotechnology, Seoul, Korea. Pectasol-C modified citrus pectin (Pect-MCP) was purchased from EcoNugenics (Santa Rosa, CA, USA). Recombinant human galectine-3 (rhGal-3) provided by Pepro Tech (NJ, USA).

MTT colorimetric assay

SKOV-3 (8000 cells/well) cells were seeded in 96-well plates in RPMI+FBS 10% and next day were treated with PTX (10, 50, 100, 250, 500, 1000 nM) and/or with Pect-MCP (0.025, 0.05, 0.1%) for 24h and 48h. In another set of experiment cells were treated with rhGal-3 (10, 100, 250, 500 ng/ml) in RPMI/FBS 0.5% for 48h. At the end of indicated incubation time, 10 µl MTT solution (5mg/ml) was added to each well followed by incubation at 37ºC for 3h, then medium was removed and formazan crystals were revealed by adding 100µL dimethylsulfoxide (DMSO) to each well, followed by gentle 10 min shaking at room temperature (RT) and absorbance (A) value was measured at 570nm with Elisa reader (Awarnesse, USA). Individual samples were analyzed in quintuplet against a background of blank wells. Cell survival from three independent experiments (mean±SD) was expressed as percentage of cell viability relative to control as follows: A value of treated cells/control cells×100. The main effect and IC_{50} of each drug PTX and Pect-MCP were obtained from MTT assay results.

Total RNA isolation and RT-PCR analysis

Isolation was performed using TRIzol according to the manufacture instruction and RNA concentration was determined using Nanodrop (Thermo scientific, Wilmington, USA).

First-strand cDNA was synthesized from 2µg total RNA by 1µl reverse transcriptase (RT) with 1µl oligodt, 1µl dNTP, 0.5µl ribonuclease inhibitor, 4µl reaction Buffer and DEPC RNase-free distilled water to reach 20µl final volume. The cDNA was amplified by polymerase chain reaction (PCR) using the following primers: hGal-3, forward: 5'-CCTCGCATGCTGATAACAATTCT-3' and reverse: 5'-TGACTCTCCTGTTGTTCTCATTGAA-3' at 57ºC. Human 18S ribosomal RNA expression was assessed as internal control with the following primers: forward- 5'- GTAACCCGTTGAACCCCATT -3'and reverse- 5'-CCATCCAATCGGTAGTAGCG-3' at 57ºC. The reaction mix contained 3µL of sample mixed with 2µl primer 100 pmol/µl, 1µl dNTP (10nM concentration), 1µl $Mgcl_2$ (50mM), 2µl PCR buffer (10×), 0.2µl Taq polymerase (5u/ml) in total volume 20µl).Each well was run in duplicate for test primer and reference (18S ribosomal RNA). The reaction for each well was carried out as follows: 95°C for 5 minutes, followed by, 57°C for 1 minute, 72°C for 1 minute ×37 cycles, then followed by 72°C for 10 minutes. Amplified products were electrophoresed on 2% agarose gels and visualized by using red safe (iNtRON, Seoul, Korea) staining under ultraviolet trans-illumination.

Detection of apoptosis and determination of cell cycle phase

The level of an apoptotic marker, cleaved caspase-3 (active form) was measured in cell lysates using a colorimetric assay kit (GenScript, NJ, USA) according to the manufacturer's instructions. Briefly, treated cells with PTX 100nM or Pect-MCP 0.1% alone or in combination or with rhGal-3 500ng/ml cells were washed twice with PBS by centrifugation at 400g for 5min, then pellets were suspended in 50µl cold lysis buffer,0.5µl DTT (1M) and 5µl PMSF (100mM) and incubated on ice for 1h with intermittent vortexing. After centrifugation at 2000g at 4°C for 1min, supernatants were transferred to a new tube and protein concentration was determined by performing Bradford assay. 100-200µg protein was mixed with 50µl of reaction buffer, 0.5µl DTT(1M), 0.25µl PMSF (100mM) and 5µl caspase-3 substrate (2 mM), incubated at 37°C for 4h and absorbance (A) value of each sample was determined at 400nm with Elisa reader (Awarnesse, USA). Wells without cells with lysis buffer alone were used as blank for non-specific A value and subtracted from test samples. Caspase-3 activity was expressed as (A value of treated/control cells)×100.

Cell cycle distribution and measurement were performed by flow cytometry. To this order, cells (65×10^4cell/ml) were seeded and day after were serum-starved for 24h before treatment of cells with PTX 100nM or Pect-MCP (0.1%) alone or in combination for 24 and 48h. The effect of rhGal-3 (500ng/ml) on cell cycle was assessed after 48h. Briefly, floating cells in medium and harvested attached cells were washed with cold phosphor-

buffered saline (PBS) and fixed with cold 70% ethanol at 4°C. After 2h, fixed cells were pelleted and stained with 10μl propodium iodide (2µg/ml) in the presence of 5μl Ribonuclease (100μg/ml) for 30 min at 37°C. About 104 cells were analyzed using a fluorescence-activated cell sorter. Data were analyzed by using win MDI2.9 software (Beckman Coulter, CA, USA). Results obtained from three independent experiments (mean±SD) were expressed as percentage of cells in different phase of cycle.

Extraction of Wharton's jelly from human umbilical cord as substrate for adhesion assay

WJE is rich in collagen type I (Bańkowski et al., 1996) which could interact and bind to Gal-3 (Lee and Juliano, 2004). Umbelical cord (UC) Wharton's jelly extract was kindly obtained from Mrs. Bahare Beigi (PhD student, School of Biology, University of Tehran). Briefly, UC were collected in a transfer medium of phosphate-buffered saline (PBS) plus 50 IU heparin and were maintained at 4°C until processing, within 24h of collection. UC were washed three times in PBS and UC artery, vein and amnion were removed then UC was cut into 1cm segments. The gelatinous tissue was excised, and minced into 0.5-1mm^3 pieces. Equal volumes of PBS were used to swell the tissue pieces with constant shaking at 4°C for 48h, and the tissue pieces were subjected to 5 freeze-thaw cycles. Samples were ruptured by high-speed dispersion on ice for 10min, and homogenized with a glass homogenizer on ice. Tissue homogenates were centrifuged at 10000g for 30min to remove debris. Protein concentration in supernatants containing Wharton's Jelly extract (WJE) was determined by performing Bradford assay. WJE (100 µl) containing mainly collagen type I, III and V was used at 10 µg/ml for coating in 96 wells plastic plates at 4°C for overnight. After washing wells twice with PBS non-specific binding sites were blocked by incubating wells with 0.2% BSA for 2h at room temperature and used for adhesion assay.

Adhesion assay

Cell adhesion assay was performed in 96-well flat bottom plates coated with WJE as described above. Briefly, cells were treated with PTX 100nM and Pect-MCP 0.1% alone or in combination for overnight then used for adhesion assay. To assess the effect of rhGal-3 on cell adhesion, immobilized rhGal-3 (100ng/ml) was used by prior incubation of rhGal-3 with WJE coated wells for 2h at 37°C before cells seeding. 20×10^3 cells were seeded to each well in triplicate and incubated for 15min at 37°C. After two times washing with PBS, cells remaining attached to the plates were fixed with 4% paraformaldehyde for 10min at room temperature, stained with a solution containing 0.5% crystal violet, 2% ethanol and 40% methanol in PBS 10min and distained with three times washing with distilled water. Then 100 µl SDS 1% was added to each well and A value was measured with Elisa reader at 600nm. Individual samples were analyzed in quadruplicate against a background of blank wells. Cell adhesion from three independent experiments (mean±SD) was expressed as percentage of adherent cells relative to control as follows: A value of treated cells/control cells×100.

Statistical analysis

Normality of nominal variables was analyzed by performing Kolmogorov–Smirnov test. Skewed and normal distributed metric variables were analyzed by Mann–Whitney U and one-way ANOVA tests, respectively that were run on SPSS version 16 (SPSS Inc., IL, USA). IC_{50} was determined by using PHARM software and combined growth-inhibitory effect for determining main effect were performed by using two-way ANOVA and Bonferroni multiple comparisons test that were run on Graph pad prism 5 (San Diego California, USA). All experiments were performed for at least tree time, and p≤0.05 was considered statistically significant.

Results

SKOV-3 cells are PTX resistant and expresses Gal-3

There was 28% (p<0.001) decreased cell viability with 100nM PTX and almost 40% reduced viability with higher PTX concentration (250, 500 and 1000 nM) after 24h (Figure 1A). PTX was more cytotoxic after 48h, there was45% with 100 nM PTX and 56% reduced cell viability with higher PTX concentration with an IC_{50}=133.7 nM (Figure 1A). Moreover, SKOV-3 cells express moderate levels of Gal-3 (Figure 1B).

Proliferative effect of rhGal-3 on SKOV-3 cells

As shown in Figure 2A, there was 41% increased viability with 500 ng/ml rhGal-3 compared to control (p<0.001) which was due to increased proliferation revealed as higher percent of cells in S phase (16.0% versus 8.6% in control, p<.01) (Figure 2B, Table 1).

Altered SKOV-3 cell cycle in the presence of Pect-MCP

Pect-MCP reduced cell viability by almost 37% (P<.001) in a dose and time independent manner which was abrogated in the presence of rhGal-3 (Figure 3) indicating a specific interaction between Pect-MCP and Gal-3. Cell cycle analysis in the presence of 0.1% PectMCP showed significant G1 arrest (74% versus 62%

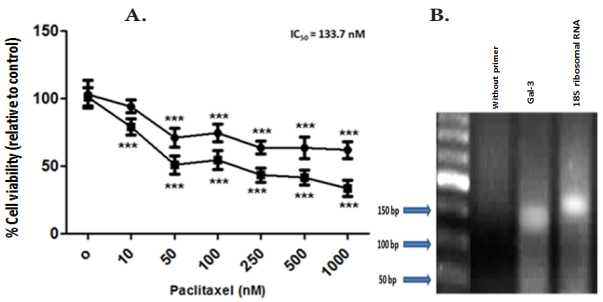

Figure 1. Dose-response curve of paclitaxel and galectine-3 RT-PCR analysis. A) Cells were treated with various concentrations of paclitaxel for 24-●-and 48h -■-. Cell viability was assessed by MTT assay. Similar dose-response was observed in increasing dose concentration of the drug added to the cells in culture. Cytotoxic effect was stronger after 48h treatment. The IC_{50} was estimated from the curve generated after 48h exposure. Values are expressed as percent (mean±SD of n=3 in triplicate); ***p<0.001 compared to control (untreated); **B)** SKOV-3 cells express moderate levels of Galectine-3. 18S Ribosomal RNA was used as internal control

in control, p<0.5) and decreased percent of cells in G2/M phase (17% versus 27.4%, p<.01) (Figure 3B, Table 1).

Higher main effect of PTX and synergistic performance of PTX and Pect-MCP

The main effect of PTX F (3,112)=90.2, p<.001 and Pect-MCP F(6,112)=86.9, p<0.001alone on cells was similar for 24h treatment. However, higher main effect of PTX F(6,112)=269.5, p<0.001 compared to Pect-MCP F(3,112)=99.3, p<0.001 was observed after 48h treatment. To assess possible interaction between Pect-MCP and PTX, experiments were performed by treatment of cells with indicated concentrations of both substances (see section material and methods) in combination followed by two way Anova analysis (Table 2). Anova analysis revealed a significant interaction between PTX and Pect-MCP with F(18,112)=3.5, p<0.001 F(18,112)= 4.4, P<.001, for 24h and 48h, respectively, Thus we can exclude additive effect and conclude a synergistic cytotoxic effect of these substances on SKOV-3 cells.

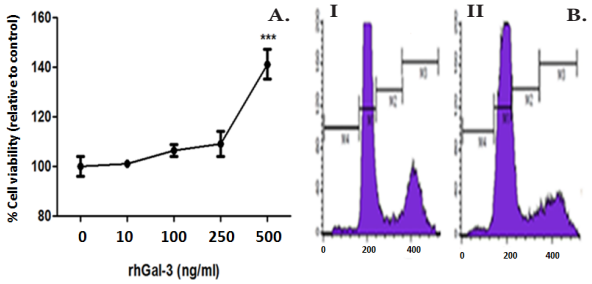

Figure 2. Evaluating the Effect of Recombinant Human Galectine-3 (rhGal-3) on Cell Viability and Progression of Cell Cycle in SKOV-3 Cell Line. A) Cells were treated with various concentrations of rhGal-3 for 48h. Cell viability was assessed by MTT assay; **B)** Cells were incubated for 48h without (I) or with (II) rhGal-3 (500 ng/mL) and cell-cycle analysis was performed by Flow Cytometry using propidium iodide (PI) staining. In each sample, 104 events were recorded and experiments were repeated three times. The percentage of cells in subG1 (M4), G0/G1 (M1), S (M2), and G2/M (M3) phases of the cell cycle was determined from FL2-A histograms using win MDI2.9 software showed in Table 1. Values are presented as percent (means±SD of n=3) cell viability compared to control; p<0.05 is interpreted to be significant, ***p<0.001

Pect-MCP sensitize SKOV-3 cells to PTX

Among different combination of PTX and Pect-MCP, the most effective combination was obtained with PTX (100nM) and Pect-MCP (0.1%) in combination (Table 2). Figure 4A showed that treatment of cells for 24h with PTX or Pect-MCP alone led to 28% and 37% decreased cell viability, respectively, versus 62% decreased cell survival in the presence of combined PTX and Pect-MCP (p<0.001). The cytotoxic effect of PTX alone or in combination with Pect-MCP was more effective after 48h treatment. There was 47% and 37% decreased cell survival with PTX or Pect-MCP, respectively, versus 71.5% reduced cell viability with combined PTX and Pect-MCP (p<0.001) (Figure 4A). Interestingly, the cytotoxic effect of PTX was reduced in presence of rhGal-3 from 48% to 36% after 48h (p<0.05) (Figure 4A).

Correspondingly, treatment of cells with PTX and Pect-MCP showed 40% number of cells in subG1 versus 2.5% in control (p<0.001) (Table 1, Figure 4B). There was 11.3% percent of cells in subG1 with PTX (100 nM) versus 2.5% in control (p<0.01) (Table 1, Figure 4B). This finding agrees with 3.9-fold increased caspase-3 activity in the presence of Pect-MCP+PTX compared to 1.6-fold with Pect-MCP alone (p<0.001) (Figure 5), however there was no significant change of capase-3 activity in PTX (100nM) treatment (Figure 5). In accordance with rhGal-3 proliferative effect (Figure 2) there was also 36% (p<0.001) decreased caspase-3 activity suggesting anti-apoptotic role of Gal-3 in SKOV-3 cells (Figure 5).

Table 1. Effect of rhGal-3, PTX and Pect-MCP Alone or in Combination on Cell Cycle Progression of SKOV-3 Cells after 48h Treatment

Condition	subG1	G1	S	G2/M
Control	2.5±1.0	61.5±2.3	8.6±3.3	27.4±3.4
rhGal-3 500ng/ml	1.3±2.5	54.1±3.3	16.2±1.9**	28.4±2.3
PTX 100nM	11.3±2.7**	23.9±1.4***	7.4±3.3	57.4±2.6***
Pect-MCP 0.1%	4.2±2.3	74.5±3.2*	4.4±2.1	16.9±2.4
PTX100 nM+Pect-MCP 0.1%	40.0±2.9***	19.5±2.0***	11.6±1.1	28.9±4.0

*p<0.05; **p<0.01; ***p<0.001

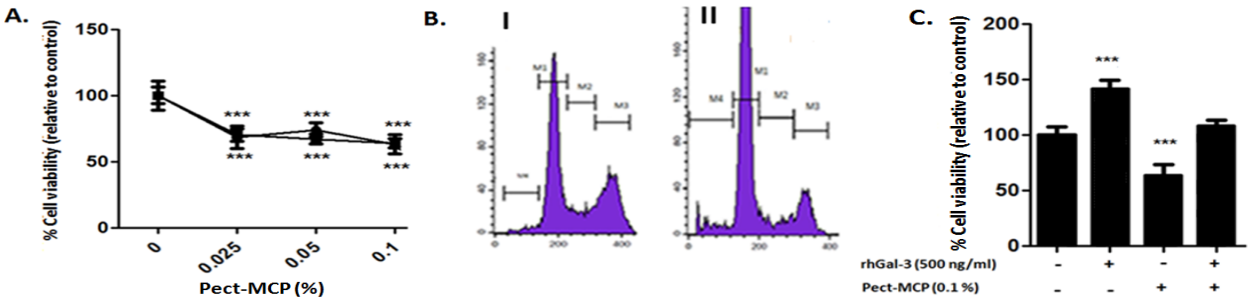

Figure 3. Effect of PectaSol-C Modified Citrus Pectin (Pect-MCP) on SKOV-3 Cell Viability and Progression of Cell Cycle in the Absence or Presence of rhGal-3. A) Cells were treated with various concentrations of Pect-MCP for 24h and 48h. Similar dose-response was observed in increasing dose concentration of the Pect-MCP added to the cells in culture; **B)** Cells were incubated for 48h I) in the absence or II) presence of Pect-MCP (0.1%) and cell-cycle analysis was performed by flow cytometry using propidium iodide (PI) staining.The percentage of cells in subG1 (M4), G0/G1 (M1), S (M2), and G2/M (M3) phases of the cell cycle was determined from FL2-A histograms using win MDI2.9 software showed in Table 1; **C)** Cells were incubated for 48h with Pect-MCP (0.1%) in the absence or presence of rhGal-3. No significant change in cell viability was detected indicating Pect-MCP specific interaction with rhGal-3. Data are presented as percent (means±SD of n=3) cell viability compared to control; ***p<0.001

Table 2. Effect of PTX and Pect-MCP Alone or in Combination on SKOV-3 Cells Viability after 24h and 48h Treatment

Condition	%cell viability (relative to control) 24h	48h	Condition	%cell viability (relative to control) 24h	48h
Control	100.0±2.1	100±2.6	PTX 250 nM	64±4.13^{***a}	41±5.06^{***a}
Pect-MCP 0.025%	68.6±4.3^{***a}	71±3.14^{***a}	PTX 250 nM+Pect-MCP 0.025%	38.8±3.91^{***a,b,c}	32±3.53^{***a,c}
Pect-MCP 0.05%	74.0±4.7^{***a}	67± 3.17^{***a}	PTX 250 nM+Pect-MCP 0.05%	43±4.23^{***a,b,c}	32±3.78^{***a,c}
Pect-MCP 0.1%	63.0±4.1^{***a}	63±3.91^{***a}	PTX 250nM+Pect-MCP 0.1%	45±4.23^{***a,b,c}	30±4.31^{***a,c}
PTX 10nM	95.0±3.9	78±3.3^{***a}	PTX 500 nM	62±3.91^{***a}	42±3.49^{***a}
PTX 10nM+Pect-MCP 0.025%	71.8±4.15^{***a,b}	63±4.21$^{***a, **b}$	PTX 500nM+Pect-MCP 0.025%	50±4.22^{***a}	31±3.71^{***a,c}
PTX 10nM+Pect-MCP 0.05%	70.0±4.63^{***a,b}	66±3.37^{***a}	PTX 500nM+Pect-MCP 0.05%	45±3.96$^{***a,c, *b}$	31±3.58^{***a,c}
PTX 10nM+Pect-MCP 0.1%	66.0±4.23^{***a,b}	51±4.18^{***a,b}	PTX 500nM+Pect-MCP 0.1%	42±4.11$^{***a,c, **b}$	27±3.76^{***a,c}
PTX 50nM	69.0±4.23^{***a}	56±4.26^{***a}	PTX 1μM	59±4.08^{***a}	33±3.51^{***a}
PTX 50nM+Pect-MCP 0.025%	69.4±4.33^{***a}	41±4.11^{***a,c}	PTX 1μM+Pect-MCP 0.025%	39±3.86$^{***a,c, **b}$	21±3.64^{***a,c}
PTX 50nM+Pect-MCP 0.05%	63.5±4.56^{***a}	46±3.33^{***a,c}	PTX 1μM+Pect-MCP 0.05%	32±4.23^{***a,b,c}	20±4.11$^{***a,c, *b}$
PTX 50nM+Pect-MCP 0.1%	60.8±3.95^{***a}	38±3.81^{***a,c}	PTX 1μM+Pect-MCP 0.1%	40±23.0$^{***a, *b, **c}$	17±3.18$^{***a,c, **b}$
PTX 100nM	72.0±4.05^{***a}	53±3.63^{***a}			
PTX 100nM+Pect-MCP 0.025%	45.4±3.88^{***a,b,c}	42±4.29^{***a,c}			
PTX 100nM+Pect-MCP 0.05%	44.0±4.21^{***a,b,c}	33±4.52^{***a,b,c}			
PTX 100nM+Pect-MCP 0.1%	38.4±23^{***a,b,c}	29±3.68^{***a,b,c}			

*p<0.05; **p<0.01; ***p<0.001.; [a]compared to control; [b]compared to PTX alone; [c]compared to Pect-MCP alone

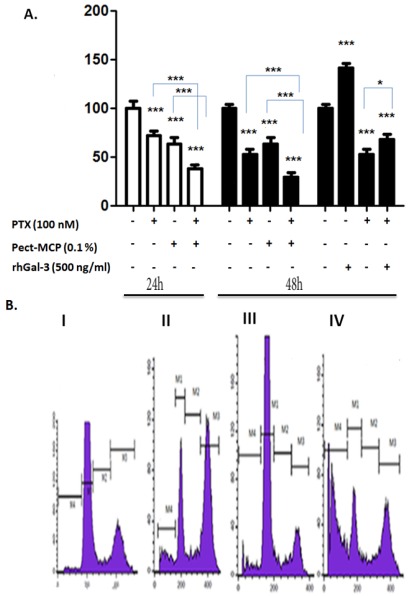

Figure 4. Effect of Paclitaxel and Pect-MCP in Combination on SKOV-3 Cell Viability. A) Cells were treated with Pect-MCP (0.1%) and 100 nM paclitaxel (PTX) for 24h ❒ and 48h ■. Pect-MCP sensitize cells to PTX by synergistic effect on reducing cell viability. Treatment of cells with combined PTX and rhGal-3 for 48h increased cell viability; **B)** Cells were incubated for 48h with Pect-MCP (0.1%) and PTX (100 nM) followed by flow-cytometry cell cycle analysis using propidium iodide (PI) staining. I) control, II) PTX alone, III) Pect-MCP alone, IV) Pect-MCP+PTX. Note increased subG1 (M4) peak in combination compared to control and each drug alone. The percentage of cells in G0/G1 (M1), S (M2), G2/M (M3) and subG1 (M4) phases of the cell cycle was determined and showed in Table 1. Data are presented as percent (means±SD of n=3) cell viability compared to control. *p<.0.05; ***p<0.001

Gal-3 affects SKOV-3 cell adhesion to collagen

In adherent cells, transition from G to S phase needs increased adherence to extracellular matrix (Zhu et al., 1996). As rhGal-3 led to increased percent of cells in S phase this has prompted us to investigate the role of Gal-3 on SKOV-3 cell adherence to collagen. In the presence of rhGal-3, there was 34% increased cell adhesion (p<0.001) compared to control (Figure 6). Correspondingly, there

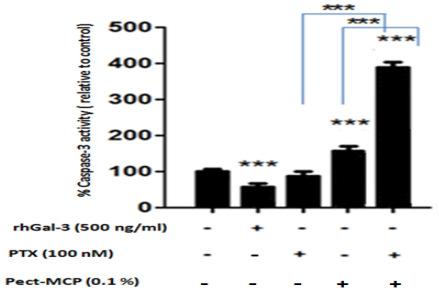

Figure 5. Evaluation of Caspase-3 Cleavage in the Presence of Pect-MCP, PTX or rhGal-3. Cells were incubated for 48h with rhGal-3 (500 ng/ml) and Pect-MCP (0.1%) or PTX (100 nM) alone or in combination. Caspase-3 activity was measured using colorimetric protease assay based on the spectrophotometric detection of the chromophore, p-nitroaniline (p-Na), after its cleavage from the labelled caspase substrates. Note increased caspase-3 activity in combination treatment compared to control and each drug alone. The presence of rhGal-3 decreased caspase-3 activity compared to control. Data are expressed as percent (means±SD of n=2 performed in triplicate) caspase-3 activity compared to control. ***p<0.001

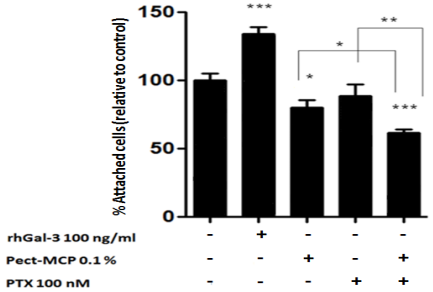

Figure 6. Effect of rhGal-3, Pect-MCP or PTX Alone or in Combination on SKOV-3 Cell-substrate Adhesion. Wells were coated with Wharton jelly extract (see Materials and Methods section). After 15 minutes incubation, non-adherent cells were washed away and the ratio of adhering cells was quantified by assessing the background-corrected absorbance at 600 nm. Presence of Gal-3 increased cell attachment compared to control and combination of PTX+Pect-MCP reduce significantly substrate-dependent cell attachment. Data are expressed as percent (means±SD of n=3) remained attached cells compared to control. *p<0.05; **p<0.01; ***p<0.001

was 20% decreased cell adhesion compared to control ($p<0.05$) in the presence of Pect-MCP (Figure 6). Although, PTX had no significant effect on cell adhesion, but when combined with Pect-MCP led to 39% decreased cell adhesion ($p<0.001$) (Figure 6).

Discussion

The early stages of ovarian cancer can be effectively treated by chemotherapy but most of the time ovarian cancer was diagnosed at late stage and unfortunately chemotherapy is not effective, because cancer cells develop resistance to chemotherapy drugs such as PTX. Therefore, it is imperative to explore novel therapeutic to improve the sensitivity of ovarian cancer cells to chemotherapy.

The present study showed for the first time that Gal-3 increases SKOV-3 ovarian cancer cells proliferation, adhesion to collagen and has anti-apoptotic effect. Moreover, inhibition of Gal-3 by Pect-MCP sensitizes ovarian cancer cells to PTX. It has been demonstrated that exogenous Gal-3 stimulates cell proliferation of primary human preadipocyte, lung fibroblast IMR-90 and endothelial cells differentiated from bone marrow mesenchymal stem cells by stimulating DNA synthesis in a dose-dependent manner (Kiwaki et al., 2007; Wan et al., 2011). In agreement with previous studies, here we showed that rhGal-3 promoted proliferation of SKOV-3 cells in a dose-dependent manner, reduced cells in G1 phase and increase number of cells in S phase. Other reports showed that Gal-3 affect Cyclin D1 expression and its inhibition induced G1 arrest by decreasing Cyclin E2, Cyclin D2 and CDK6 and increasing cell cycle inhibitor p21Cip (Lin et al., 2002; Streetly et al., 2010).

This study showed anti-apoptotic effect of Gal-3 on SKOV-3 cells which was reversed in the presence of Pect-MCP. In agreement with this finding other studies reported that Gal-3 imparts resistance to apoptosis in breast, bladder and prostate cancer (Choi et al., 2004; Oka et al., 2005; Wang et al., 2010), by Bcl-2 up-regulation and inhibition of Gal-3 induced caspase-3 activity (Wang et al., 2010). Another report showed that use of Pect-MCP as a blocker of cell surface Gal-3 could induce apoptosis in prostate cancer by suppression of MAPK pathway (Yan and Katz, 2010). Moreover, combination of Pect-MCP and chemotherapeutic drugs sensitized prostate cancer cells to antineoplastic drugs by decreasing Bcl-2 expression (Tehranian et al., 2012). Similarly, knockout of Gal-3 expression by RNA interference enhanced cytotoxic effect of Paclitaxel in SKOV-3 cells (Kim et al., 2011). The present study demonstrated for the first time that Pect-MCP may be a useful therapeutic drug in combination therapy of ovarian cancer.

For most cells, the ability to proliferate depends on two signals. First, cells need to detect that they are appropriately positioned within the tissue. This information is provided by integrins surface receptors that sense the extracellular matrix and connect it to the cytoskeleton which activate many signaling cascades and influence cell responses to other stimuli Second, cells require growth factors and cytokines for proliferation (Lee and Juliano, 2004). When cells lose their normal cell–matrix interactions,the cell cycle is arrested led to initiation of a specific form of caspase-mediated programmed cell death, known as anoikis (Frisch and Ruoslahti, 1997). Tumor cells have developed a variety of strategies to bypass or overcome anoikis, cancer cells afford to increase survival time in the absence of matrix attachment, facilitate eventual re-attachment and increase their proliferation in secondary site (Frisch and Ruoslahti, 1997).

In this study, we showed for the first time an increased number of attached cells to coated wells with WJE in the presence of rhGal-3. It was previously reported that Gal-3 has a critical role in cell adhesion by binding to glycoprotein component of extracellular matrix such as laminin, fibronectin, colagen I and IV (Ochieng et al., 1998). Likely, it has been demonstrated that Gal-3 increased neutrophil cells adhesion to laminin and fibronectin (Kuwabara and Liu, 1996). In accordance with these results use of Pect-MCP led to reduced cell adhesion and combined Pect-MCP+PTX enhanced this effect. It should be noted that SKOV-3 cells was reported to be anoikis resistant (Sher et al., 2009), thus based on anti-apoptotic effect of Gal-3 and enhancement of cell attachment with rhGal-3, it may be tempting to speculate that this molecule could play a critical role to help SKOV-3 cells to bypass anoikis pathway. Further experiments may warrant this hypothesis.

Here, PTX cell treatment induced G2/M arrest and increased percentage of cells in subG1 phase without any significant change in caspase-3 activity. It is well known that taxols such as PTX stabilizes the spindle during mitosis, thereby blocking cell division leading to inhibition of cell proliferation and apoptosis (Ahn et al., 2004). PTX has been shown to induce caspase-3 enzymatic activity in other human carcinoma cell lines, including the acute myelocytic leukemia cell line HL-60, as well as lung and colon cancer cell lines 35-37 (Perkins et al., 1998; Goncalves et al., 2000; Weigel et al., 2000). However, this drug has an unusual mode of action in human ovarian carcinoma SKOV-3 cells, a mechanism that does not require caspase-3 activation (Ahn et al., 2004). Although, treatment of SKOV-3 cells with taxol resulted in Bcl-2 phosphorylation and mitochondrial depolarization, cytochrome-C was not released and pro-caspase-3 was not activated (Ahn et al., 2004). It has been demonstrated that treatment of SKOV-3 cells with taxol, resulted in the translocation of apoptosis-inducing factor (AIF) from the mitochondria to the nucleus via the cytosol (Ahn et al., 2004). AIF is a phylogenetically conserved mitochondrial intermembrane flavoprotein that has the ability to induce apoptosis via a caspase independent pathway (Loeffler et al., 2001). AIF plays an important role in inducing nuclear chromatin condensation as well as large-scale DNA fragmentation (approximately 50 kb), and is essential for programmed cell death (Loeffler et al., 2001) Thus it seems that effect of taxol on caspase-3 activation is cell type specific.

As PTX has serious side effects, any agent that may lead to more effective cytotoxic effect or use of lower dose of this agent may be an interesting candidate for combination therapy. Our data showed that Pect-MCP

could be a strong and effective tool to this combination therapy. The present study demonstrated that Pect-MCP combined to low concentration of PTX could increase significantly caspase-3 activity and percentage of cells in subG1compared to control or each drug alone. Moreover, specific inhibition of Gal-3 by Pect-MCP was confirmed by finding that exogenously added rhGal-3 decreased basal caspase-3 activity and subsequent percent of cells in subG1 phase. In addition, co-treatment of rhGal-3 and PTX led to reduced cytotoxic effect of PTX suggesting that Gal-3 may play an important role in ovarian cancer chemoresistance. Taken together, our study demonstrated that Pect-MCP can sensitize ovarian cancer cells to paclitaxel through inducing apoptosis, which then led to accumulation of cells in subG1 and G1 phases and cleavage of caspase-3, suggesting that the combined use of Pect-MCP and PTX may be an effective way to decrease the dose of paclitaxel taken. Further experiments may clarify the important signaling pathway and key molecules influenced by combined use of Pect-MCP and PTX in human ovarian cancer.

Acknowledgements

This work was supported in part by grant number 28940/1/6 from University College of Science, University of Tehran.

References

Ahn HJ, Kim YS, Kim JU, et al (2004). Mechanism of taxol-induced apoptosis in human SKOV3 ovarian carcinoma cells. *J Cell Biochem*, **91**, 1043-52.

Bae J, Lim MC, Choi JH, et al (2009). Prognostic factors of secondary cytoreductive surgery for patients with recurrent epithelial ovarian cancer. *J Gynecol Oncol*, **20**, 101-6.

Banerjee S, Gore M (2009). The future of targeted therapies in ovarian cancer. *Oncologist*, **14**, 706-16.

Bańkowski E, Sobolewski K, Romanowicz L, et al (1996). Collagen and glycosaminoglycans of Wharton's jelly and their alterations in EPH-gestosis. *Eur J Obstet Gynecol Reprod Biol*, **66**, 109-17.

Choi JH, Chun KH, Raz A, et al (2004). Inhibition of N-(4-hydroxyphenyl) retinamide-induced apoptosis in breast cancer cells by galectin-3. *Cancer Biol Ther*, **3**, 447-52.

Chumworathayi B (2013). Personalized cancer treatment for ovarian cancer. *Asian Pac J Cancer Prev*, **14**, 1661-4.

Loeffler M, Daugas E, Susin SA, et al (2001). Dominant cell death induction by extramitochondrially targeted apoptosis-inducing factor. *FASEB J*, **215**, 758-67.

Elola MT, Wolfenstein-Todel C, Troncoso MF, et al (2007). Galectins: matricellular glycan-binding proteins linking celladhesion, migration, and survival. *Cell Mol Life Sci*, **64**, 1679-700.

Glinsky VV, Kiriakova G, Glinskii OV, et al (2009). Synthetic galectin-3 inhibitor increases metastatic cancer cell sensitivity to taxol-induced apoptosis *in vitro* and *in vivo*. *Neoplasia*, **11**, 901-9.

Goncalves A, Braguer D, Carles G, et al (2000). Caspase-8 activation independent of CD95/CD95-L interaction during paclitaxel-induced apoptosis in human colon cancer cells (HT29-D4). *Biochem Pharmacol*, **60**, 1579-84.

Inohara H, Raz A (1994). Effects of natural complex carbohydrate (citrus pectin) on murine melanoma cell properties related to galectin-3 functions. *Glycoconj J*, **11**, 527-32.

Inohara H, Akahani S, Raz A (1998). Galectin-3 stimulates cell proliferation. *Exp Cell Res*, **245**, 294-302.

Iurisci I, Tinari N, Natoli C, et al (2000). Concentrations of galectin-3 in the sera of normal controls and cancer patients. *Clin Cancer Res*, **6**, 1389-93.

Jemal A, Siegel R, Ward E, et al (2006). Cancer statistics. *CA Cancer J Clin*, **56**, 106-30.

Kim HR, Lin HM, Biliran H, et al (1999). Cell cycle arrest and inhibition of anoikis by Galectin-3 in human breast epithelial cells. *Cancer Res*, **59**, 4148-54.

Kim MK, Sung CO, Do IG, et al (2011). Overexpression of Galectin-3 and its clinical significance in ovarian carcinoma. *Int J Clin Oncol*, **16**, 352-8.

Kiwaki K, Novak CM, Hsu DK (2007). Galectin-3 stimulates preadipocyte proliferation and is up-regulated in growing adipose tissue. *Obesity*, **15**, 32-9.

Kuwabara I, Liu FT (1996). Galectin-3 promotes adhesion of human neutrophils to laminin. *J Immunol*, **156**, 3939-44.

Lee JW, Juliano R (2004). Mitogenic signal transduction by integrin- and growth factor receptor-mediated pathways. *Mol Cells*, **17**, 188-202.

Lin HM, Pestell RG, Raz A, et al (2002). Galectin-3 enhances cyclin D1 promoter activity through SP1 and a cAMP-responsive element in human breast epithelial cells. *Oncogene*, **21**, 8001-10.

Nangia-Makker P, Nakahara S, Hogan V, et al (2007). Galectin-3 in apoptosis, a novel therapeutic target. *J Bioenerg Biomembr*, **39**, 79-84.

Ochieng J, Leite-Browning ML, Warfield P (1998). Regulation of cellular adhesion to extracellular matrix proteins by galectin-3. *Biochem Biophys Res Commun*, **246**, 788-91.

O'Driscoll L, Linehan R, Liang YH, et al (2002). Galectin-3 expression alters adhesion, motility and invasion in a lung cell line (DLKP), in vitro. *Anticancer Res*, **22**, 3117-25.

Oka N, Nakahara S, Takenaka Y, Fukumori T, et al (2005). Galectin-3 inhibits tumor necrosis factor-related apoptosis-inducing ligand-induced apoptosis by activating Akt in human bladder carcinoma cells. *Cancer Res*, **65**, 7546-53.

Perkins C, Kim CN, Fang G, et al (1998). Overexpression of Apaf-1 promotes apoptosis of untreated and paclitaxel- or etoposide-treated HL-60 cells. *Cancer Res*, **8**, 4561-6.

Pienta KJ, Naik H, Akhtar A, et al (1995). Inhibition of spontaneous metastasis in a rat prostate cancer model by oral administration of modified citrus pectin. *J Natl Cancer Inst*, **87**, 348-53.

Platt D, Raz A (1992). Modulation of the lung colonization of B16-F1 melanoma cells by citrus pectin. *J Natl Cancer Inst*, **84**, 438-42.

Sher I, Adham SA, Petrik J, et al (2009). Autocrine VEGF-A/KDR loop protects epithelial ovarian carcinoma cells from anoikis. *Int J Cancer*, **124**, 553-61.

Streetly MJ, Maharaj L, Joel S, et al (2010). GCS-100, a novel galectin-3 antagonist, modulates MCL-1, NOXA, and cell cycle to induce myeloma cell death. *Blood*, **115**, 3939-48.

Tehranian N, Sepehri H, Mehdipour P, et al (2012). Combination effect of PectaSol and Doxorubicin on viability, cell cycle arrest and apoptosis in DU-145 and LNCaP prostate cancer cell lines. *Cell Biol Int*, **36**, 601-10.

van den Brûle FA, Berchuck A, Bast RC, et al (1994). Differential expression of the 67-kD laminin receptor and 31-kD human laminin-binding protein in human ovarian carcinomas. *Eur J Cancer*, **30**, 1096-9.

Wan SY, Zhang TF, Ding Y (2011). Galectin-3 enhances proliferation and angiogenes of endothelial cells differentiated from bone marrow mesenchymal stem cells. *Transplant Proc*, **43**, 3933-8.

Wang Y, Nangia-Makker P, Balan V (2010). Calpain activation through galectin-3 inhibition sensitizes prostate cancer cells to cisplatin treatment. *Cell Death Dis*, **1**, 101.

Wani MC, Taylor HL, Wall ME, et al (1971). The isolation and structure of taxol, a novel antileukemic and antitumor agent from Taxus brevifolia. *J Am Chem Soc*, **93**, 2325-7.

Weigel TL, Lotze MT, Kim PK, et al (2000). Paclitaxel-induced apoptosis in nonsmall cell lung cancer cell lines is associated with increased caspase-3 activity. *J Thorac Cardiovasc Surg*, **119**, 795-803.

Wongkham S, Junking M, Wongkham C, et al (2009). Suppression of galectin-3 expression enhances apoptosis and chemosensitivity in liver fluke-associated cholangiocarcinoma. *Cancer Sci*, **100**, 2077-84.

Yan J, Katz A (2010). PectaSol-C Modified Citrus Pectin Induces Apoptosis and Inhibition of Proliferation in Human and Mouse Androgen Dependent and -Independent Prostate Cancer Cells. *Integr Cancer Ther*, **9**, 197-203.

Zhao Q, Barclay M, Hilkens J, et al (2010). Interaction between circulating galectin-3 and cancer-associated MUC1 enhances tumour cell homotypic aggregation and prevents anoikis. *Molecular Cancer*, **9**, 154.

Zhu X, Ohtsubo M, Böhmer RM, et al (1996). Adhesion-dependent cell cycle progression linked to the expression of cyclin D1, activation of cyclin E-cdk2, and phosphorylation of the retinoblastoma protein. *J Cell Biol*, **133**, 391-403.